Analysis of Macular Thickness Deviation Maps for Diagnosis of Glaucoma

Bingnan Zhou[1], Farnaz Mohammadi[2], Jung S. Lim[1], Negin Forouzesh[1], Hassan Ghasemzadeh[3], and Navid Amini[1,2]

[1] California State University Los Angeles, Los Angeles CA 90032, USA
[2] University of California Los Angeles, Los Angeles CA 90095, USA
[3] Arizona State University, Tempe AZ 85281, USA

namini@calstatela.edu

Abstract. There is a growing number of studies showing that analysis of macular parameters provides additional information about ganglion cell loss in glaucoma and compliments traditional markers of glaucoma. In this paper, we develop an image processing pipeline for the macular thickness deviation maps generated by Heidelberg Spectralis optical coherence tomography (OCT) to evaluate the information within the macular measurements for diagnosing glaucoma. Logistic regression is applied to analyze features extracted from the deviation maps and the strength of their relationship with the diagnosis of glaucoma. Our experimental results show that the proportion of regions with thickness significantly below the normative range in the nerve fiber layer thickness deviation maps can be used to detect glaucoma with an accuracy of up to 70.16%. Moreover, the ganglion cell layer deviation maps also possess significant diagnostic ability for detection of glaucoma, which can be combined with the traditional assessments of the optic nerve head and peripapillary retinal nerve fiber layer to improve the reliability of glaucoma diagnosis.

Keywords: Glaucoma, Macula, Feature Selection, Logistic Regression, Machine Learning.

1 Introduction

Glaucoma is a group of disorders that progressively damage the optic nerve and is currently considered the second leading cause of blindness in the world. According to prevalence studies, as of 2020, 79.6 million people worldwide suffer from glaucoma [1], and it is believed that the number will increase to more than 111 million by 2040 [2]. Due to the increasing prevalence of glaucoma, there are numerous research studies seeking to effectively detect glaucoma to overcome the economic, psychological, and societal challenges associated with glaucoma. It is widely believed that glaucoma mainly affects three areas of the human retina, namely optic nerve head (ONH), peripapillary retinal nerve fiber layer, and the macula.

The diagnosis of glaucoma has traditionally been based on the discovery of ONH damage in the form of cupping and the thinning of the peripapillary retinal nerve fiber layer (RNFL) as shown by the red and green circles in Fig. 1; however, the sole utility of these traditional markers falls short of providing accurate glaucoma diagnosis [1], [2]. It has been reported that the macula (delineated by the blue circle in Fig. 1) offers several potential physiological and anatomical advantages for glaucoma detection and management [3], [4].

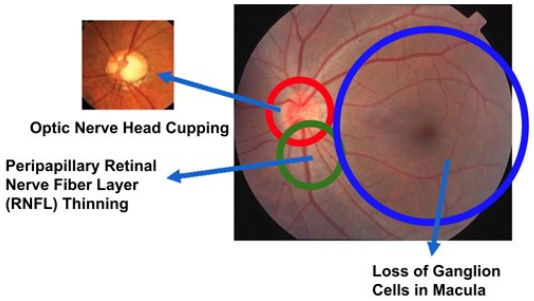

Fig. 1. The optic nerve head (red circle), the peripapillary retinal nerve fiber layer (green circle), and macula (blue circle) are retinal areas that are mostly affected by glaucoma.

Specifically, the thickness of the inner layers of the macula has been shown to not only correlate with traditional markers in glaucoma, but also to provide additional information that can complement the diagnostic ability of the traditional markers [4]–[6] The thickness of the three innermost retinal layers in the macular region may represent a surrogate indicator of the degeneration and death of retinal ganglion cells, given the prominent distribution of these cells within the macular region [7], [8]. These three layers include the retinal nerve fiber, ganglion cell, and inner plexiform layers, which contain, respectively, the axons, cell bodies, and dendrites of the ganglion cells.

Optical coherence tomography (OCT) is a non-invasive, micrometer-scale, and cross-sectional imaging technology for biological tissue. It has been widely used for retinal imaging in ophthalmology as it provides high-resolution information of the cross-section and surface of retina. With OCT, tiny tissues such as the retinal layers can be quantified and visualized. In this study, we focus on the diagnosis power of the macula; we investigate the extent of information that resides in the macula and study the relationship between such information and glaucoma diagnosis. With the progression of glaucoma and degeneration of ganglion cells, the first three layers of retina in macula will thin out. We develop an image processing pipeline to extract quantitative features related to the thickness of inner retinal layers from the macular deviation maps generated by Heidelberg Spectralis OCT. The pipeline is mainly used to process the macular deviation maps of each subject and extract the diagnostic data to form the dataset required for the study. We then use logistic regression as our classifier to analyze subjects' macular data and discover the relationship between each macular parameter (feature) and glaucoma diagnosis.

Feature-based machine learning techniques have been extensively used for glaucoma detection. Summary statistics extracted by clinicians such as RNFL thickness, mean deviation measurements from visual field tests, and computer-vision based detection of optic cup-to-disc ratio from fundus images of the eye have been used to aid in automating glaucoma detection [9] with accuracy rates on the order of 87% [9]. Machine learning techniques such as support vector machines (the effort by Dey and Bandyopadhyay [10]), decision trees (the study by Huang and Chen [11]), random forest classifiers (the work of Sugimoto and colleagues [12]), *k*-nearest neighbors (investigation by Balasubramanian and associates [13]), *k*-means clustering (by Ayub et al. [14]), linear discriminant analysis (study by Bambo and co-investigators [15]), and Bayesian (the investigation by Bowd et al. [16]) classifiers can be used to detect presence of disease once these summary statistics or features are extracted. However, the initial features are typically human-selected disease markers, resulting in datasets that are small in size, increasing the likelihood of overfitting (obtaining high accuracy on specific datasets without general applicability of an approach), as well as potentially losing important aspects of the data [17] [18]. The above-mentioned studies lack a normative database for the features that they fed as inputs to learning algorithms for glaucoma detection. We argue that comparison of these features (e.g., macular thickness measurements) with a reference, normative database of normal subjects enhances their diagnostic power and improves the visualization of structural defects associated with glaucoma.

The present study is designed to determine the diagnostic performance of commercially available macular thickness deviation maps obtained by Spectralis OCT for glaucoma detection. The deviation maps consist of inner retinal layer thickness parameters. The normality cutoffs and ranges of these thickness parameters are determined by comparisons to Heidelberg Engineering's age-matched normative database.

To the best of our knowledge, this is the first effort to evaluate the diagnostic performance of macular deviation maps in glaucoma. Based on promising results from experiments on 955 deviation maps of 93 glaucomatous eyes and 98 normal eyes, we expect the macular deviation maps and their corresponding normality ranges will improve the ability to detect glaucoma, which will potentially lead to more effective management of this disease. The rest of this paper is organized as follows. Section 2 presents the image processing pipeline for deriving macular features from the deviation maps and methods for evaluation of those features for the detection of glaucoma. Section 3 covers the experimental results and corresponding discussions. Finally, the conclusions of this study are presented in Section 4.

2 Methods

2.1 Macular OCT Imaging

OCT devices acquire structural information of the posterior segment of the eye. Many one-dimensional scans (A-scans or depth reflectivity profiles) are performed at several depths to create a two-dimensional cross-sectional image called a B-scan. Macular B-scans, if acquired closely and rapidly, can be translated into a volumetric image of the

posterior segment centered on the macula. These B-scans include structures such as vitreous, retina, choroid, and sclera (See Fig. 2). Among these structures, retina is where the eye's visual receptors and various ocular tissues are located. As such, OCT devices usually set their image acquisition properties in such a way that retina can be imaged reliability and with the highest signal-to-noise ratio among these four structures.

Spectralis OCT has developed a specific software tool that provides automated delineation and thickness measurements of 10 retinal layers. The anterior (top) three layers form the inner retina, while the posterior (bottom) seven layers compose the outer retina. It is well established that glaucoma results in a thinning of the inner retina, i.e., decreased retinal nerve fiber layer (RNFL), ganglion cell layer (GCL), and inner plexiform layer (IPL) thickness; however, no changes in outer retinal layer thicknesses have been reported [19], [20]. Therefore, in this study, we only target the thickness levels of RNFL GCL, IPL, or their combinations, such as ganglion cell-inner plexiform layer (GCIPL) and the full retinal thickness (FRT) in the macular region as indicated in Fig. 2.

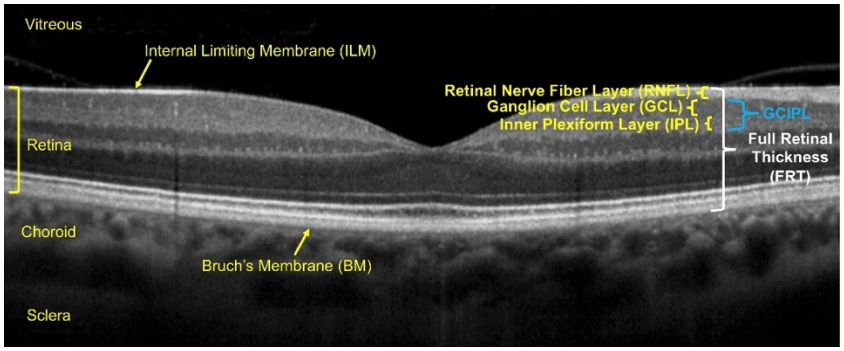

Fig. 2. A macular OCT B-Scan visualizes structures in the posterior segment of the eye, which include vitreous, retina, choroid, and sclera in an anterior to posterior order. Full retinal thickness (FRT) as well as the thickness of the first three layers of retina, i.e., retinal nerve fiber layer (RNFL), ganglion cell layer (GCL), and inner plexiform layer (IPL), or their combinations (e.g., GCIPL) can be used as predictors of glaucoma.

The original OCT scans were acquired from 98 normal and 93 glaucomatous eyes using the Posterior Pole Algorithm of the Spectralis OCT, which acquires 61 horizontal B-scans at approximately 120 μm apart, extending across a 30°×25° area of the macula. Each B-scan consists of 768 A-scans, with the acquisition process being repeated 9-11 times to decrease speckle noise [21].

A scanning laser ophthalmoscopy (SLO) technology is integrated into most OCT devices to achieve *en face* fundus images, which constitute a useful complement to the cross-sectional B-scans. Fig. 3 shows an *en face* fundus image and a cross-sectional OCT B-scan corresponding to the location of the green line on the *en face* image. B-scan images are approximately perpendicular to the retinal surface, while *en face* fundus images are nearly parallel to the retinal surface providing a direct, front view of the retina. Integration of an SLO technology into the OCT device can help localize and visually interpret the key OCT measurements such as thickness values.

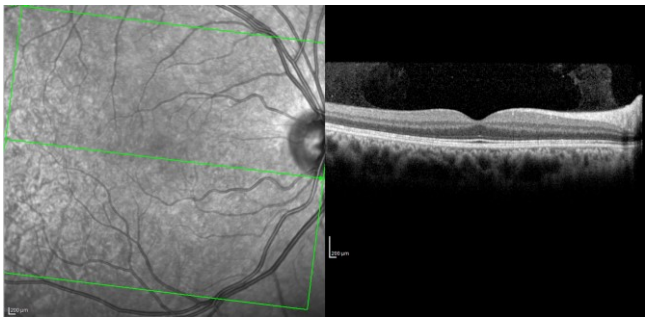

Fig. 3. An *en face* fundus image (left) and a cross-sectional, macular OCT B-scan (right). The green line one the *en face* fundus image shows the exact location of the B-scan.

Macular thickness measurements for different layers are performed for each individual B-scan. The thickness measurements can be color-coded and overlaid on top of the *en face* fundus image as illustrated in Fig. 4(A). With the help of reference normative databases, Spectralis OCT is able to generate a deviation map to highlight the probability that the thickness measurements of each macular retinal layer are within or outside of normal limits [22]. As shown in Fig. 4(B), the deviation maps reveal regions and associated patterns in specific retinal layers that have statistically significant thinner or thicker values. Comparison of thickness measurements with the reference database enhances their diagnostic value. The deviation maps highlight the probability of measurements that are not within normal limits.

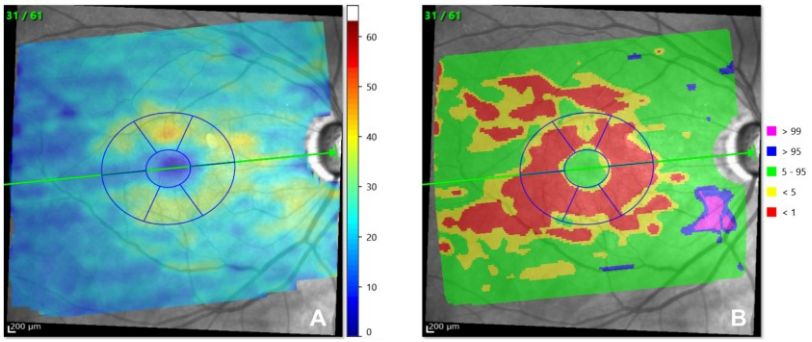

Fig. 4. (A) An example of Heidelberg Spectralis *en face* fundus image overlaid with thickness map. The thickness map is color-coded according to the ganglion cell layer's thickness in µm in this example. (B) Corresponding deviation map overlaid on same *en face* fundus image. The deviation map is a color-coded indication of normative data comparison. Percentile limits of the normal distribution are computed by the device. The meaning of the *n*th percentile is that *n* percent of normal subjects from the normative database have a thickness value (ganglion cell thickness in this example) less than or equal to this value.

For each normal, healthy eye in the normative database, thickness at each macular location and for each inner retinal layer is measured. From these measurements, the age-adjusted percentiles of the eyes in the database are determined. These age-adjusted percentiles form the basis for highlighting a result as being within or outside the normal

limits. The meaning of the *n*th percentile is that *n* percent of normal subjects from the database sample have a thickness of less than or equal to this value.

A macular deviation map highlights deviation from normal values; in Spectralis macular deviation maps, five ranges of thickness deviations are coded with five different colors from thickness deviation less than 1% to greater than 99% of thickness values of the normal eyes that belong to the normative database of Spectralis OCT. Regions where the thickness deviation lies between 5-percentile and 95-percentile of normal thickness values are considered normal regions and shown in green. Regions with values between 1-percentile and 5-percentile of thickness values of normal eyes are yellow regions, and red regions represent regions with thickness values less than 1-percentile of the normal thickness values. This means that less than 1% of normal eyes from the normative database have a thickness value less than or equal to that of the red regions. Spectralis OCT, also visualizes supernormal (above normal) regions. Supernormal regions contain thickness values greater than the 95-percentile (e.g., >95% or 99% cut-offs). If a macular location has a thickness value between 95-percentile and 99-percentile, it will be shown in blue. Lastly, locations that have very high thickness values to the extent that only 1% of normal eyes in the normative database have thickness above that value will be shown in pink.

2.2 Macular Deviation Map Processing

The normative reference database and the exact methods for the derivation of percentiles and adjusting the probabilities for age and perhaps other factors are proprietary to Heidelberg Engineering, the manufacturer of Spectralis OCT. Nevertheless, we can take deviation maps as inputs to our diagnostic pipeline and define features based on them for detection of glaucoma. The proportion of pixels with each of the five color-codes can be used as features or predictors of glaucoma or its severity. It should be noted that these colors correspond with probabilities of deviation from the normal range for each acquired pixel in the deviation map based on a comparison with an age-matched control group of normal, healthy eyes.

The common approach of calculating each proportion is to count the number of pixels of each of the five color-codes on the deviation map. The proportions will be calculated for two focus areas: (1) the entire posterior pole imaged by the OCT device (the entire rectangular scan area shown in Fig. 4(A)), and (2) the macular elliptical ring (annulus) developed on the macular scan with OCT software (See Fig. 4(C)). The latter focus area is centered around the fovea (central part of macula) and has the highest density of retinal ganglion cells [23]. OCT devices choose to exclude the foveal area where the retinal layers are very thin and difficult to detect accurately. That is why the focus area is effectively between two concentric ellipses forming an elliptical ring. The OCT device divides the elliptical ring into six sectors, as shown in Fig. 4.

As shown in Fig. 5, in order to effectively quantify the deviation maps, the OCT image processing pipeline converts an input deviation map, such as the one shown in Fig. 5(A), into the formats shown in Fig. 5(B) and Fig. 5(C), where all the areas other than the focus areas are masked. We then calculate the proportion of each thickness

deviation for each format and form a dataset from those calculations. Therefore, the kernels of the proposed pipeline include masking redundant pixels and ellipse detection.

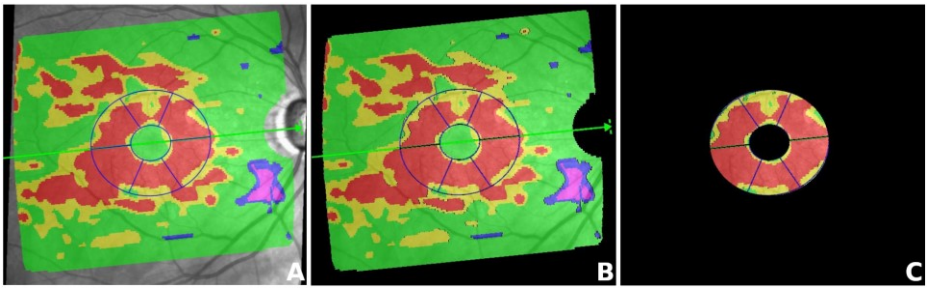

Fig. 5. Illustration of original and processed macular deviation maps. (A) Original deviation map. (B) Deviation map with focus on the entire rectangular scan area. (C) Deviation map of the elliptical ring (annulus) of the ganglion cell layer. In this example, the deviation maps are based on the thickness of the ganglion cell layer.

Masking Redundant Pixels. Since the only elements that we need to quantify are the five color-codes corresponding to the five thickness deviation levels, the first stage of the proposed pipeline is to generate masked deviation maps from the original deviation map. Redundant pixels can be masked by setting color thresholds in five ranges, denoted as C_1, C_2, C_3, C_4, and C_5, where each range includes all possible colors of each thickness deviation level. If a pixel is not within these ranges, the pipeline will classify such a pixel as a redundant pixel whose value will be converted to black. Fig. 6 outlines the flowchart for the masking process.

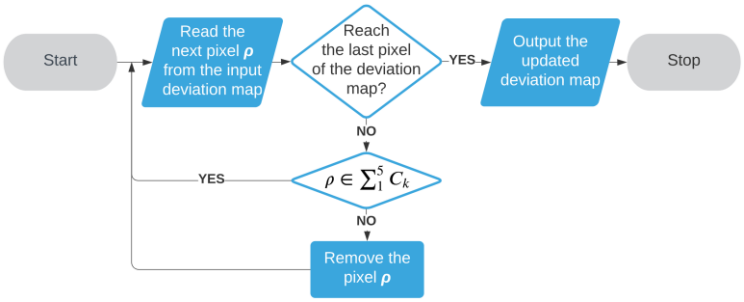

Fig. 6. Flowchart for masking the redundant pixels on macular deviation maps.

Ellipse Detection and Fitting. As mentioned earlier, the elliptical ring in each macular deviation map is the area with the highest density of retinal ganglion cells. However, the location of the two ellipses that form the elliptical ring depends on various characteristics of an eye, such as the curvature of the retina, and it varies from subject to subject. On each deviation map, two ellipses that bound the elliptical ring are extracted using a least-square ellipse fitting algorithm [24]–[26]. Briefly, an ellipse can be considered a conic section, formed by the intersection of a plane with a right circular cone. The general equation that can be used to represent any conic section can be written as:

$$Ax^2 + Bxy + Cy^2 + Dx + Ey + F = 0, \quad (1)$$

where (x, y) represent coordinates of points lying on the ellipse, and A, B, C, D, E, and F are the coefficients of the ellipse.

If there is a set S of coordinates (at least 5) located on the boundary of the ellipse, through applying the least squares criterion, the objective function can be constructed as follows:

$$\sum_{k=1}^{m}(Ax_k^2 + Bx_k^2y_k^2 + Cy_k^2 + Dx_k + Ey_k + 1)^2 = 0, \quad (2)$$

where (x_k, y_k) is the coordinate from the set S, and m is the number of points to which we fit an ellipse.

There are a number of techniques to detect the boundary of the ellipse to obtain the set S, such as the Hough transform [27]. The proposed pipeline integrates a simple coordinate range test along with the Hough transform to determine five points the boundary of the ellipse. After plugging in all coordinates from the set S, the corresponding system of linear equations can be solved with the partial derivative of each parameter, thereby fitting the ellipse.

2.3 Dataset Overview

There is a total of 955 macular deviation maps from 191 eyes (98 normal eyes and 93 glaucomatous eyes) in the database. Through applying the proposed image processing pipeline, every macular deviation map generates six features including the proportions of pink, blue, yellow, and red regions, as well as the proportion of abnormal regions (i.e., proportion of regions that are red or yellow) and the proportion of supernormal regions (i.e., proportion of regions that are blue or pink). These two union (cumulative) features can be calculated by summing the proportions of yellow (<5% thickness deviation) and red (<1% thickness deviation) regions, and the proportions of blue (>95% thickness deviation) and pink (>99% thickness deviation) regions, respectively. The normal (green) region of the deviation maps forms more than 75% of the data composition. Furthermore, the normal region is complementary to the other four color-codes. Therefore, we did not include the proportion of green region in the dataset.

For each eye, five macular deviation maps are available in the database. These include the FRT deviation map, the GCIPL thickness deviation map, the GCL thickness deviation map, the IPL thickness deviation map, and the RNFL thickness deviation map. For each deviation map, the six features discussed above are derived for both entire rectangular scan area and the elliptical ring of the macula. Accordingly, in total, 60 features will be extracted and maintained for each eye. The outcome of our analysis is a binary outcome indicating the presence or absence of glaucoma [28].

2.4 Machine Learning for Feature Evaluation

To sort the 50 features based on their relevance and contribution to the binary outcome, we create a logistic regression model comprising all eyes, but considering one feature

at a time [29], [30]. As can be seen in Fig. 7, each classification model is based on one feature. Leave-one-out cross-validation is used to train and evaluate the model. For the correlation and ranking of each feature, besides the classification accuracy based on the corresponding classification model, factors such as true positive (TP), true negative (TN), false positive (FP) and false negative (FN) are also considered to gain a comprehensive assessment.

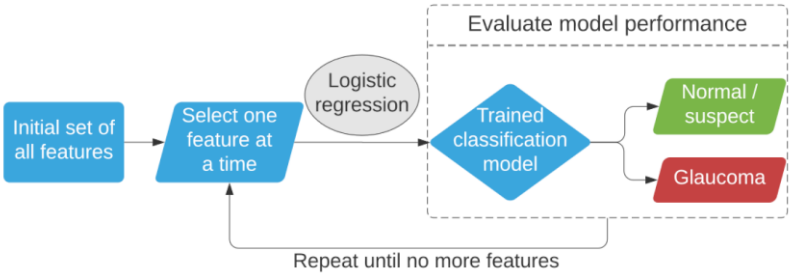

Fig. 7. Flowchart of automatic glaucoma classification with logistic regression.

3 Results and Discussions

Univariate logistic regression models, comprising 98 normal eyes and 93 glaucomatous eyes, are used to evaluate the strength of the relationship between individual features (as independent variables) and the binary outcome of the study, i.e., presence or absence of glaucoma (as the dependent variable). The ranking of the ten most relevant features to binary classification is given in the highlight table of Fig. 8. The values in the table are the average accuracy of the logistic regression classification model of the feature in the first column. If the value appears in the column "Elliptical Ring," it means that the corresponding feature comes from the macular elliptical ring. If the accuracy value appears in the column titled "Entire Rectangle," the feature is derived from the entire rectangular scan area in deviation maps.

The features listed in the first row of the highlight table and the subsequent charts follow the naming convention: the name starts with the name of the retinal layer to which the feature belongs, and the "Rectangle" or "Ring" identification indicates that the feature comes from the entire rectangular scan area in deviation maps or the central elliptical ring of the retinal layer, respectively; lastly, the third word of a feature's name represents the thickness deviation level or levels of a specific retinal layer. For example, "red" means that the thickness is less than that of the bottom 1% of the eyes in the normative database (i.e., <1% cutoff). Similarly, "abnormal" means the cumulative regions of red/yellow, meaning that the thickness is less than that of the bottom 5% or less than that for the bottom 1% of eyes in the normative database (i.e., <5% or <1% cutoffs).

The highlight table indicates that the best performing feature is the proportion of abnormal regions on the RNFL deviation map of the entire rectangular scan area. Such a feature alone can achieve accuracy of 69% in detection of glaucoma. Furthermore, we can observe that none of top six prominent features belongs to the elliptical ring

defined by the OCT device. Another observation is that the RNFL-related features from the central elliptical ring do not appear among the best-performing features.

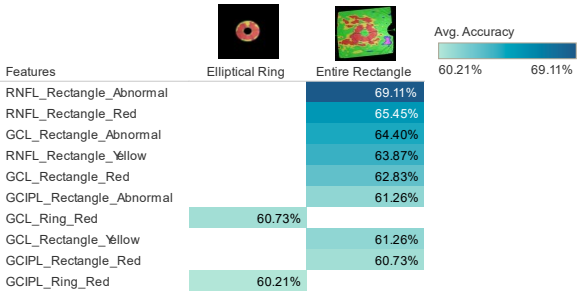

Fig. 8. Highlight table of the top 10 best-performing features.

As shown before, the proportion of abnormal regions within the entire rectangular scan area in RNFL thickness deviation maps is the most prominent feature for detection of glaucoma. The univariate logistic regression classifier based on the proportion of red regions as its single predictive feature delivers the accuracy of 64.45% in detecting glaucoma (Fig. 9(A)). If we cumulatively consider red/yellow regions as one feature (i.e., <5% or <1% cutoffs), the univariate logistic regression classifier achieves the accuracy of 69.11% (Fig. 9(B)). We achieve a slightly better accuracy of 70.16% with a bivariate logistic regression with two independent features being the proportion of red regions and the proportion of yellow regions (Fig. 9(C)).

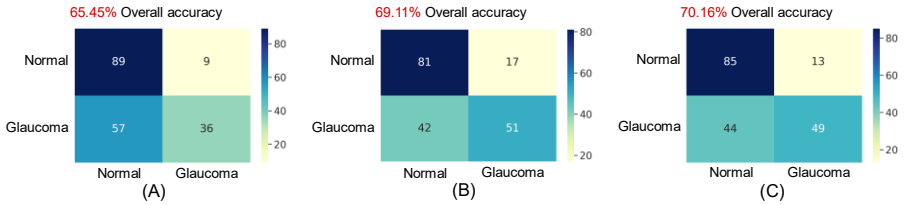

Fig. 9. Comparison of three logistic regression models for glaucoma detection. (A) Confusion matrix based on the proportion of red regions within the entire rectangular scan area in RNFL thickness deviation maps. (B) Confusion matrix based on the cumulative red/yellow regions (i.e., abnormal regions) (C) Confusion matrix based on independent proportions of red and yellow regions, utilized as two predictive features.

Our experimental results indicate that there is significant information in regard to glaucoma detection in the macula and specifically within the macular thickness deviation maps generated by OCT devices. Furthermore, the features defined based on the macular elliptical ring, despite containing the highest density of retinal ganglion cells, fall behind the features defined in the elliptical ring (e.g., RNFL) in terms of glaucoma diagnosis power. It should be noted that our results do not imply that one should make diagnostic decisions solely based on the macula. In fact, there are several pieces to the glaucoma puzzle. However, our findings can help develop better diagnostic tools for detection of glaucoma.

4 Conclusions

Optical coherence tomography (OCT) allows for non-invasive imaging of glaucomatous structural damage involving the optic nerve head, peripapillary retinal nerve fiber layer, and the macular region. In this paper, we develop an image processing pipeline for the macular thickness deviation maps generated by Heidelberg Spectralis optical coherence tomography (OCT) to evaluate the information within the macular measurements for the diagnosis of glaucoma. Logistic regression is then applied to analyze features extracted from the deviation maps and the strength of their relationship with diagnosis of glaucoma. Our experimental results show that the proportion of regions with thickness significantly below the normative range in the nerve fiber layer thickness deviation maps can be used to detect glaucoma with an accuracy of up to 70.16%. Moreover, the ganglion cell layer deviation maps possess significant diagnostic ability for detection of glaucoma, which can be combined with the traditional assessments of the optic nerve head and peripapillary retinal nerve fiber layer to improve the reliability of glaucoma diagnosis.

References

[1] M. Michelessi *et al.*, "Optic nerve head and fibre layer imaging for diagnosing glaucoma," *Cochrane Database of Systematic Reviews*, vol. 2015, no. 11. 2015.

[2] O. Tan *et al.*, "Detection of Macular Ganglion Cell Loss in Glaucoma by Fourier-Domain Optical Coherence Tomography," *Ophthalmology*, 2009.

[3] A. Miraftabi *et al.*, "Macular SD-OCT outcome measures: Comparison of local structure-function relationships and dynamic range," *Investig. Ophthalmol. Vis. Sci.*, 2016.

[4] Z. Chen, Y. Wang, G. Wollstein, M. De Los Angeles Ramos-Cadena, J. Schuman, and H. Ishikawa, "Macular GCIPL Thickness Map Prediction via Time-Aware Convolutional LSTM," in *Proceedings - International Symposium on Biomedical Imaging*, 2020.

[5] H. Raja, T. Hassan, M. U. Akram, and N. Werghi, "Clinically Verified Hybrid Deep Learning System for Retinal Ganglion Cells Aware Grading of Glaucomatous Progression," *IEEE Trans. Biomed. Eng.*, 2021.

[6] N. Amini, S. G. Miremadi, and M. Fazeli, "A hierarchical routing protocol for energy load balancing in wireless sensor networks," in *Canadian Conference on Electrical and Computer Engineering*, 2007.

[7] H. Ishikawa, D. M. Stein, G. Wollstein, S. Beaton, J. G. Fujimoto, and J. S. Schuman, "Macular segmentation with optical coherence tomography," *Investig. Ophthalmol. Vis. Sci.*, 2005.

[8] N. Amini, A. Vahdatpour, F. Dabiri, H. Noshadi, and M. Sarrafzadeh, "Joint consideration of energy-efficiency and coverage-preservation in microsensor networks," *Wirel. Commun. Mob. Comput.*, 2011.

[9] H. Muhammad *et al.*, "Hybrid Deep Learning on Single Wide-field Optical Coherence tomography Scans Accurately Classifies Glaucoma Suspects," *J. Glaucoma*, 2017.

[10] A. Dey and S. Bandyopadhyay, "Automated Glaucoma Detection Using Support Vector Machine Classification Method," *Br. J. Med. Med. Res.*, 2016.

[11] M. L. Huang and H. Y. Chen, "Glaucoma classification model based on GDx VCC measured parameters by decision tree," *J. Med. Syst.*, 2010.

[12] K. Sugimoto, H. Murata, H. Hirasawa, M. Aihara, C. Mayama, and R. Asaoka, "Cross-sectional study: Does combining optical coherence tomography measurements using the 'Random Forest' decision tree classifier improve the prediction of the presence of perimetric deterioration in glaucoma suspects?," *BMJ Open*, 2013.

[13] K. Balasubramanian, N. P. Ananthamoorthy, and K. Gayathridevi, " Automatic Diagnosis and Classification of Glaucoma Using Hybrid Features and k -Nearest Neighbor ," *J. Med. Imaging Heal. Informatics*, 2018.

[14] J. Ayub *et al.*, "Glaucoma detection through optic disc and cup segmentation using K-mean clustering," in *2016 International Conference on Computing, Electronic and Electrical Engineering, ICE Cube 2016 - Proceedings*, 2016.

[15] M. P. Bambo *et al.*, "Diagnostic capability of a linear discriminant function applied to a novel Spectralis OCT glaucoma-detection protocol," *BMC Ophthalmol.*, 2020.

[16] C. Bowd *et al.*, "Bayesian machine learning classifiers for combining structural and functional measurements to classify healthy and glaucomatous eyes," *Investig. Ophthalmol. Vis. Sci.*, 2008.

[17] S. Maetschke, B. Antony, H. Ishikawa, G. Wollstein, J. Schuman, and R. Garnavi, "A feature agnostic approach for glaucoma detection in OCT volumes," *PLoS One*, 2019.

[18] and W. X. Kaiser, William J., Majid Sarrafzadeh, Hyduke Noshadi, Shaun S. Ahmadian, Hagop Hagopian, Navid Amini, Mars Lan, Jonathan S. Woodbridge, "Method of assessing human fall risk using mobile systemst," 8,823,526, 2014.

[19] D. C. Hood, A. S. Raza, C. G. V. de Moraes, J. M. Liebmann, and R. Ritch, "Glaucomatous damage of the macula," *Progress in Retinal and Eye Research*. 2013.

[20] K. Takayama *et al.*, "A novel method to detect local ganglion cell loss in early glaucoma using spectral-domain optical coherence tomography," *Investig. Ophthalmol. Vis. Sci.*, 2012.

[21] G. Mahmoudinezhad *et al.*, "Detection of Longitudinal GCIPL Change: Comparison of Two Spectral Domain Optical Coherence Tomography Devices," *Am. J. Ophthalmol.*, 2021.

[22] Heidelberg Engineering, "Enhanced Features, Enhanced Diagnostics," 2020. .

[23] C. A. Curcio and K. A. Allen, "Topography of ganglion cells in human retina," *J. Comp. Neurol.*, 1990.

[24] P. L. Rosin, "A note on the least squares fitting of ellipses," *Pattern Recognit. Lett.*, vol. 14, no. 10, pp. 799–808, 1993.

[25] A. Fitzgibbon, M. Pilu, and R. B. Fisher, "Direct least square fitting of ellipses," *IEEE Trans. Pattern Anal. Mach. Intell.*, vol. 21, no. 5, 1999.

[26] H. Yousefi, F. Mohammadi, N. Mirian, and N. Amini, "Tuberculosis Bacilli Identification: A Novel Feature Extraction Approach via Statistical Shape and Color Models," in *Proceedings - 19th IEEE International Conference on Machine Learning and Applications, ICMLA 2020*, 2020.

[27] D.H.Ballard, "Generalizing the Hough transform to detect arbitrary shapes," *Pattern Recognition*, vol. 13, no. 2. pp. 111–122, 1981.

[28] S. S. Ahmad, "Glaucoma suspects: A practical approach," *Taiwan Journal of Ophthalmology*, vol. 8, no. 2. 2018.

[29] C. Y. J. Peng, K. L. Lee, and G. M. Ingersoll, "An introduction to logistic regression analysis and reporting," *J. Educ. Res.*, vol. 96, no. 1, 2002.

[30] C.-Y. J. Peng and T.-S. H. So, "Logistic Regression Analysis and Reporting: A Primer," *Underst. Stat.*, vol. 1, no. 1, 2002.